Carcinogenesis vol.28 no.11 pp.2412–2418, 2007
doi:10.1093/carcin/bgm164
Advance Access publication July 17, 2007

Glucuronidation of PhIP and *N*-OH-PhIP by UDP-glucuronosyltransferase 1A10

Ryan W.Dellinger[1,3], Gang Chen[1,4], Andrea S.Blevins-Primeau[1,3], Jacek Krzeminski[2,3], Shantu Amin[1,2,3] and Philip Lazarus[1,3,4,*]

[1]Cancer Prevention and Control Program and [2]Chemical Carcinogenesis and Chemoprevention Program, Penn State Cancer Institute and [3]Department of Pharmacology and and [4]Department of Public Health Sciences, Penn State University College of Medicine, 500 University Drive, Hershey, PA 17033, USA

[*]To whom correspondence should be addressed. Tel: +1 717 531 5734; Fax: +1 717 531 0480;
Email: plazarus@psu.edu

The UDP-glucuronosyltransferase (UGT) 1A10 is an extra-hepatic enzyme that plays an important role in the glucuronidation of a variety of endogenous and exogenous substances and is expressed throughout the aerodigestive and digestive tracts. Two classes of carcinogens that target the colon, heterocyclic amines (HCAs) and polycyclic aromatic hydrocarbons, are known to be detoxified by the UGT family of enzymes. Recently, our laboratory demonstrated that UGT1A10 has considerably more activity against polycyclic aromatic hydrocarbons *in vitro* than any other UGT family member. In this study, we focused on the glucuronidation of the HCA, 2-amino-1-methyl-6-phenylimidazo[4,5-*b*]pyridine (PhIP), and its bioactivated metabolite, *N*-hydroxy-2-amino-1-methyl-6-phenylimidazo[4,5-*b*]pyridine (*N*-OH-PhIP). We demonstrated that UGT1A10 exhibited a significantly higher glucuronidation rate against PhIP and *N*-OH-PhIP than any other UGT family member *in vitro* using whole-cell homogenates of HEK293 cells over-expressing individual UGTs. Kinetic analysis revealed a 9- and 22-fold higher level of activity for UGT1A10 homogenates as compared with the next most active UGT, UGT1A1, against *N*-OH-PhIP as determined by maximum rate/apparent Michaelis constant (V_{max}/K_M) at the N3 and N^2 positions, respectively. The polymorphic UGT1A10^{139Lys} variant exhibited a 2- to 16-fold decrease in glucuronidation activity against PhIP and *N*-OH-PhIP, as compared with the wild-type UGT1A10^{139Glu} isoform. These data suggest that UGT1A10 is the most active UGT against PhIP and *N*-OH-PhIP and that UGT1A10 may play an important role in susceptibility to HCA-induced colon cancer.

Introduction

The carcinogen 2-amino-1-methyl-6-phenylimidazo[4,5-*b*]pyridine (PhIP[1]) is the most mass abundant heterocyclic amine (HCA) found in cooked meat (1,2) as well as being present in tobacco smoke (3). Studies in rodents have demonstrated that PhIP induces tumors in the colon, prostate and breast (4). PhIP is metabolically activated by cytochrome P450 enzymes yielding *N*-hydroxy-2-amino-1-methyl-6-phenylimidazo[4,5-*b*]pyridine (*N*-OH-PhIP), which can be subsequently esterified by acetyltransferases and sulfotransferases generating carcinogenic species that can react with DNA to form adducts (4). Both PhIP and *N*-OH-PhIP are also known to be detoxified by glucuronidation at both the N^2 and N3 positions (5,6). The major conjugated metabolite found in human urine is *N*-OH-PhIP-N^2-glucuronide and increased levels of this metabolite corresponded to lower levels of DNA adducts found in the colon of individuals exposed to PhIP at a low dose (7). This finding suggests that the more efficient individuals are at detoxifying *N*-OH-PhIP, the less susceptible they may be to colon cancer.

Abbreviations: HCA, heterocyclic amine; HPLC, high-pressure liquid chromatography; K_M, apparent Michaelis constant; *N*-OH-PhIP, *N*-hydroxy 2-amino-1-methyl-6-phenylimidazo[4,5-*b*]pyridine; PhIP, 2-amino-1-methyl-6-phenylimidazo[4,5-*b*]pyridine; UGT, UDP-glucuronosyltransferase; V_{max}, maximum rate.

The UDP-glucuronosyltransferase (UGT) superfamily of enzymes catalyze the glucuronidation of a variety of endogenous compounds such as bilirubin and steroid hormones, as well as xenobiotics such as drugs and environmental carcinogens (8–12). The UGTs are membrane-bound proteins that conjugate glucuronic acid to substrates making them more hydrophilic and easily excreted. In this manner, UGTs are integrally involved in the detoxification of many carcinogens, the clearance of drugs and the metabolism of a variety of endogenous compounds (13). Based upon structural and amino acid sequence homology, UGTs are classified into several families and subfamilies (14). UGT2B family members are derived from independent genes located in chromosome 4, whereas the entire UGT1A family is derived from a single gene locus in chromosome 2. The UGT1A locus codes for nine functional proteins that differ only in their N-terminus as a result of alternate splicing of independent exon 1 regions to a shared C-terminus encoded by exons 2–5 (9,15).

Previous studies on the glucuronidation of the dietary carcinogen PhIP and its bioactivated metabolite *N*-OH-PhIP demonstrated that both compounds are glucuronidated at the N^2 and N3 positions (5,6,16). In two separate reports, the major conjugated metabolite found in human urine was *N*-OH-PhIP-N^2-glucuronide although significant levels of *N*-OH-PhIP-N3-glucuronide and PhIP-N^2-glucuronide were also observed (16,17). Furthermore, increased levels of *N*-OH-PhIP-N^2-glucuronide in urine corresponded to lower levels of DNA adducts found in the colon of individuals exposed to PhIP (7). Thus, it is important to ascertain the UGTs responsible for both PhIP and *N*-OH-PhIP glucuronidation.

Previous studies have suggested that UGT1A1 plays an important role in the glucuronidation of both PhIP (5) and *N*-OH-PhIP (6,16). The goal of the present study was to comprehensively examine the glucuronidating activities of the UGT superfamily of enzymes against both PhIP and *N*-OH-PhIP *in vitro*. Evidence is presented indicating that UGT1A10 is the most active UGT family member against both PhIP and *N*-OH-PhIP and that the polymorphic variant UGT1A10^{139Lys} has significantly decreased glucuronidation activity against both PhIP and *N*-OH-PhIP. Also, evidence is presented demonstrating that UGT1A10 is found primarily in the non-microsomal fraction of the cell, which could account for its relatively low or undetectable activity against a number of substrates, including PhIP and *N*-OH-PhIP, in previous studies (6,16).

Materials and methods

Chemicals and materials

PhIP was obtained from the National Cancer Institute Chemical Carcinogen Repository (Midwest Research Institute, Kansas City, MO). *N*-OH-PhIP was synthesized in the Organic Synthesis Facility of the Penn State Cancer Institute (Penn State University College of Medicine, Hershey, PA). Alamethicin and UDP-glucuronic acid were purchased from Sigma (St Louis, MO) and Dulbecco's Modified Eagle's Medium, fetal bovine serum and Geneticin (G418) were purchased from Gibco (Carlsbad, CA). The human UGT1A Western blotting kit that includes the anti-UGT1A polyclonal antibody was purchased from Gentest (Woburn, MA) whereas the anti-β-actin monoclonal antibody and anti-calnexin polyclonal antibody were obtained from Sigma. UGT1A1- and UGT1A10-over-expressing baculosomes were purchased from Gentest.

Cell lines stably over-expressing individual UGT family members (including the UGT1A10^{139Lys} cell line) were previously described (11,18–20). Briefly, cell lines over-expressing UGTs 1A1, 1A4, 1A6 and 2B7 were kind gifts from Brian Burchell (University of Dundee, Dundee, UK) or Tom Tephly (University of Iowa, Iowa City, IA). For UGTs 1A3, 1A7, 1A8, 1A10, 2B4, 2B10, 2B11, 2B15 and 2B17, cDNAs were obtained by reverse transcription–polymerase chain reaction from total RNA isolated from various human tissues known to express the UGT of interest (e.g. liver for hepatic UGTs and esophageal or laryngeal RNA for extra-hepatic UGTs 1A7, 1A8 and 1A10). The individual UGT cDNAs were cloned into pcDNA3.1 TOPO mammalian expression plasmid (Invitrogen, Carlsbad, CA) and transfected into HEK293 cells (purchased from American Type Culture Collection, Rockville, MD) by

electroporation. Cells stably over-expressing the individual UGT were selected for with G418 (Invitrogen).

Homogenate and microsomal preparation

Cell homogenates were prepared by re-suspending pelleted cells in Tris-buffered saline (25 mM Tris base, 138 mM NaCl and 2.7 mM KCl; pH 7.4) and subjecting them to three rounds of freeze–thaw prior to gentle homogenization. Cell homogenates (5–20 mg protein/ml) were stored at −70°C in 100 µl aliquots. Total cell homogenate protein concentrations were determined using the BCA assay from Pierce Biotechnology (Rockford, IL) after protein extraction using standard protocols. Microsomes were prepared from homogenates by centrifugation at 10 000*g* for 20 min at 4°C followed by ultracentrifugation of the supernatant at 100 000*g* for 1 h at 4°C to pellet the microsomal fraction. The pellet was then re-suspended in Tris-buffered saline and stored in 100 µl aliquots at −70°C.

Western blot analysis

Levels of UGT1A protein in UGT-over-expressing cell lines were measured by western blot analysis using the anti-UGT1A antibody (1:5000 dilution as per the manufacturer's instructions), whereas housekeeping protein levels were assayed using a 1:5000 dilution of β-actin or calnexin. Proteins were detected by chemiluminescence using the SuperSignal West Dura Extended Duration Substrate (Pierce Biotechnology). Secondary antibodies supplied with the Dura ECL kit (anti-rabbit and anti-mouse) were used at 1:3000. UGT1A protein levels were quantified against a known amount of human UGT1A protein (100 ng, supplied in the western blotting kit provided by Gentest) by densitometric analysis of X-ray film exposures (5 s to 2 min exposures) of western blots using a GS-800 densitometer with Quantity One software (Bio-Rad, Hercules, CA). Quantification was made relative to the levels of β-actin or calnexin observed in each lane (also quantified by densitometric analysis of western blots as described above). X-ray film bands were always below densitometer saturation levels as indicated by the densitometer software. Relative UGT1A protein levels are reported as the mean of three independent western blot experiments, with western blot analysis performed using the same UGT1A-containing cell homogenates used for activity assays.

Glucuronidation assays

The rate of glucuronidation by cell homogenates was determined essentially as described previously (19,21,22). Cell homogenate (300 µg protein) was incubated with alamethicin for 10 min on ice. The reaction was carried out (200 µl final volume) in 50 mM Tris–HCl (pH 7.5), 10 mM $MgCl_2$, 4 mM UDP-glucuronic acid and 125 µM PhIP or *N*-OH-PhIP at 37°C for 90 min. For glucuronidation rate determinations, substrate concentrations, cell homogenate protein levels and incubation times for individual assays were chosen to maximize levels of detection within a linear range of uptake and were similar to established protocols (21,22). For kinetic analysis, incubations were performed using 20 µg protein of UGT-over-expressing cell homogenate, with the maximum rate (V_{max}) normalized to UGT levels in the respective cell line based upon western blot analysis of protein expression for that line. PhIP or *N*-OH-PhIP concentrations ranged between 1–1000 µM, a range that encompassed the apparent Michaelis constant (K_M) for all conditions tested. Reactions were terminated by the addition of an equal volume of 100% acetonitrile on ice. Reaction mixtures were then concentrated in a Speed Vac to a final volume of 200µl and 100 µl was then analyzed by high-pressure liquid chromatography (HPLC). Glucuronidation assays were analyzed by HPLC as described previously (11,18,21). Briefly, a Beckman Coulter System Gold (Fullerton, CA) HPLC with an Aquasil 4 µm C18 analytical column (4.6 × 250 mm, Thermo, Bellefonte, PA) was used to analyze reactions at 316 nm. The gradient elution conditions were as follows: starting with 100% buffer A (90% 100 mM KH_2PO_4, pH 5.0 and 10% acetonitrile) for 10 min, a subsequent linear gradient to 70% B (90% acetonitrile) >20 min was then performed and maintained for 10 min. The elution flow rate was 1.0 ml/min. Untransfected HEK293 cells were used periodically as a negative control. Experiments were always performed in triplicate as independent assays. GraphPad Prism 4 software (GraphPad Software, San Diego, CA) was employed to calculate kinetic values. Assays using UGT1A-over-expressing microsomes or baculosomes were performed as described above.

Mass spectrometry

N^2- and N3-glucuronides were separated and collected on an HPLC as described above with some modifications. A TSK-GEL ODS-80 TM 5µm (25 cm × 4.6 mm) column (Tosoh Bioscience, Montgomeryville, PA) was used with the following conditions: starting with 85% buffer A for 5 min, a subsequent linear gradient to 70% B >20 min was then performed and maintained for 10 min. The elution flow rate was 1.0 ml/min. Collected fractions were dried using a Speed Vac and re-suspended in methanol. Fifty microliters of each fraction was re-injected on HPLC to ensure only a single peak was collected. An Applied Biosystems 4000 Q Trap (triple quadrupole) mass spectrometer (Foster City, CA) was used to characterize individual glucuronides as described previously (5,6). Spray probe temperature was set at 400°C, ionization voltage at 5000 V, the orifice and the ring at 31 V and 190 V, respectively. Data were acquired with a dwell time of 400 ms, a pause time of 5 ms and a scan time of 1.2 s. The transitions used for analysis were 417 → 241 for *N*-OH-PhIP-N^2-glucuronide, 417 → 225 for *N*-OH-PhIP-N3-glucuronide and 401 → 225 for both the PhIP-N^2-glucuronide and the PhIP-N3-glucuronide.

Statistical analysis

The Student's *t*-test (two-sided) was used for comparing rates and kinetic values of glucuronide formation for the $UGT1A10^{139Glu}$ and $UGT1A10^{139Lys}$ isoforms against the different substrates examined in this study.

Results

Glucuronidation rates of individual UGT family members against PhIP and N-OH-PhIP in vitro

While only UGTs 1A1, 1A4, 1A6 and 1A9 were examined in previous studies against PhIP (5), all known UGTs except UGTs 1A5 and 2B28 were tested against PhIP in the present analysis using whole-cell homogenates from HEK293 cells stably over-expressing individual UGTs. Reaction products were measured by HPLC and ultraviolet detection at 316 nm. As shown in Figure 1, the PhIP-glucuronide peak pattern for UGT1A1 and UGT1A4 observed in the present study shows the larger peak to be peak 2 (retention time 12.6 min) for UGT1A1 (panel A) and peak 1 (retention time 11.8 min) for UGT1A4 (panel B). Neither peak was present when PhIP was run alone (panel C). Since previous studies reported that UGT1A1 forms primarily the PhIP-N^2-glucuronide whereas UGT1A4 predominantly forms the PhIP-N3-glucuronide (5), this is consistent with peak 1 being the PhIP-N3-glucuronide and peak 2 being the PhIP-N^2-glucuronide. Consistent with previous studies, UGTs 1A1, 1A4 and 1A9 all exhibited glucuronidating activity against PhIP at both the N^2 and N3 positions whereas UGT1A6 exhibited no activity (Table I).

The only other UGT that exhibited glucuronidating activity against PhIP was UGT1A10 (Table I). PhIP-N^2-glucuronide (peak 2) was the predominant glucuronide formed by UGT1A10 cell homogenates (Figure 1, panel D). To confirm that UGT1A10 was forming glucuronides of PhIP, mass spectrometry was performed on peak 1 (Figure 1, panel E) and peak 2 (Figure 1, panel F) after individual collection. For both peaks, the mass 401 $[M + H]^+$ was shown to fragment to a mass of 225 [M + H-glucuronic acid]. This is consistent with previous reports of PhIP-glucuronides using authentic standards (17).

After normalizing for UGT1A protein expression as determined by western blot analysis (Figure 2), UGT1A10 exhibited a higher relative N^2-glucuronide rate against PhIP than any other UGT tested (Table I). The order of glucuronidation rate against PhIP at the N^2 position was 1A10 > 1A1 > 1A9 > 1A4, whereas the order of glucuronidation rate at the N3 position was 1A4 > 1A10 > 1A1 > 1A9 (Table I). All the other UGTs tested in this study (1A3, 1A6, 1A7, 1A8, 2B4, 2B7, 2B10, 2B11, 2B15 and 2B17) showed no activity against PhIP.

All UGT family members (except 1A5 and 2B28) were then tested for activity against *N*-OH-PhIP. Previous studies have shown that four glucuronides are possible for *N*-OH-PhIP (5). The two major glucuronides formed *in vitro* with human liver microsomes and found in human urine are the *N*-OH-PhIP-N^2-glucuronide and the *N*-OH-PhIP-N3-glucuronide (6,16), whereas the other two minor glucuronides remain uncharacterized and were shown to be produced by UGT1A4, UGT1A9 and UGT2B10 *in vitro* (5,6). Consistent with previous studies (16), the *N*-OH-PhIP-glucuronide HPLC peak ratio was similar for UGT1A10 and UGT1A1, with peak 1 (retention time 21.1 min) being the major peak observed and peak 2 (retention time 22.1 min) the minor peak (Figure 3, panels A and B). Since previous studies have demonstrated that UGTs 1A1 and 1A10 primarily form the *N*-OH-PhIP-N^2-glucuronide (6,16), this is consistent with peak 1 being the *N*-OH-PhIP-N^2-glucuronide and peak 2 being the *N*-OH-PhIP-N3-glucuronide. Neither peak was present when *N*-OH-PhIP was run alone (Figure 3, panel C). To confirm that UGT1A10 was forming glucuronides of *N*-OH-PhIP, mass spectrometry was

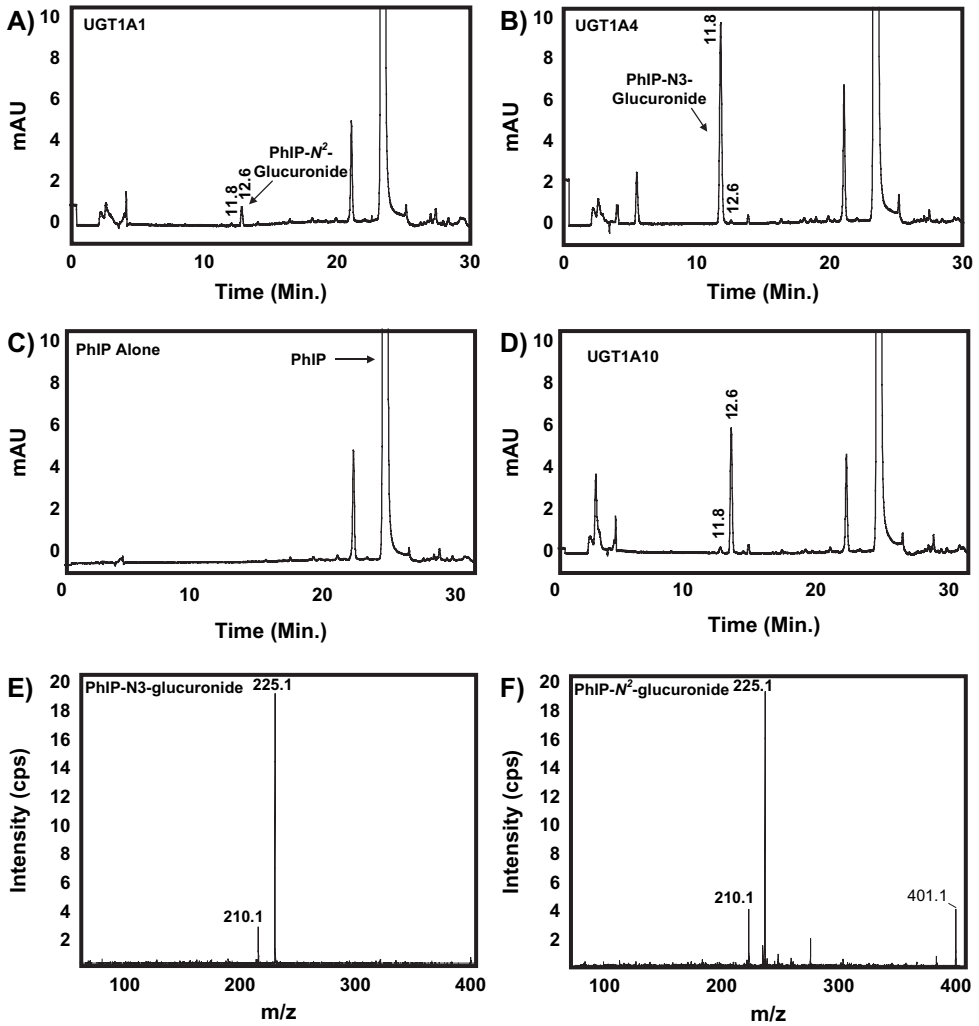

Fig. 1. Representative HPLC traces of PhIP-glucuronide separation and detection. All assays were performed using 125 μM PhIP and incubated for 90 min at 37°C. (**A**) HPLC trace using 300 μg protein of UGT1A1-over-expressing cell homogenates; PhIP-N^2-glucuronide is indicated. (**B**) HPLC trace using 300 μg protein of UGT1A4-over-expressing cell homogenates; PhIP-N3-glucuronide is indicated. (**C**) HPLC trace of PhIP alone; PhIP is indicated. (**D**) HPLC trace of incubations using 300 μg protein of UGT1A10-over-expressing cell homogenates. (**E**) Mass spectral analysis of peak 1 (retention time 11.8 min). (**F**) Mass spectral analysis of peak 2 (retention time 12.6 min).

performed on peak 1 (Figure 3, panel D) and peak 2 (Figure 3, panel E) after individual collection. For peak 1, the mass 417 $[M + H]^+$ was shown to fragment with a major ion of 241 [M + H-glucuronic acid-OH]$^+$. For peak 2, the mass 417 was shown to fragment with a major ion of 225 [M + H-glucuronic acid]$^+$. These fragment patterns are consistent with previous reports using authentic standards for the *N*-OH-PhIP-glucuronides and confirm the identity of peak 1 as the *N*-OH-PhIP-N^2-glucuronide and peak 2 as the *N*-OH-PhIP-N3-glucuronide (6,17).

As shown in Table I, several UGT1A enzymes exhibited glucuronidating activity against *N*-OH-PhIP at both the N^2 and N3 positions. Interestingly, only UGT1A4 produced minor previously uncharacterized *N*-OH-PhIP-glucuronide peaks (data not shown) that had been observed in previous studies (6). After normalizing for UGT1A protein expression (Figure 2), the order of glucuronidation activity against *N*-OH-PhIP at the N^2 position was 1A10 > 1A1 > 1A4 > 1A8 > 1A9 > 1A3 > 1A7 and at the N3 position was 1A10 > 1A1 > 1A9 ≥ 1A3 ≥ 1A8 > 1A4 > 1A7 (Table I). Similar to previous studies, no activity was observed for UGT1A6 and all the UGT2B family members tested (2B4, 2B7, 2B10, 2B11, 2B15 and 2B17) against *N*-OH-PhIP at either the N^2 or N3 positions. Of the UGT cell lines that did not exhibit activity against PhIP or *N*-OH-PhIP in this study, all have been shown to be active against other substrates using this assay system in previous studies (11,18–20). The only exceptions are the recently characterized UGT2B10- and UGT2B11-over-expressing cell lines, and the UGT2B10 line was shown to be active against a variety of substrates in recent studies (G. Chen, R. Dellinger, D. Sun, T. Spratt and P. Lazarus, in preparation).

The most active UGT against *N*-OH-PhIP at both the N^2 and N3 positions in the present study was, therefore, UGT1A10 (Table I), and these results were obtained using whole-cell homogenates from stably over-expressing HEK293 cells. This contrasts with previous studies where UGT1A10 from over-expressing baculosomes was suggested to exhibit low levels of activity (16) against *N*-OH-PhIP, whereas microsomal fractions from UGT1A10-over-expressing cells were shown to be inactive (6). To better address the differences observed between homogenates (present study) versus microsomes (6), relative UGT protein levels were assessed in microsomes versus homogenates in UGT1A1- and UGT1A10-over-expressing cell lines. As shown in Figure 4, UGT1A1 and UGT1A10 exhibited similar levels of expression in whole-cell homogenates prepared from their respective UGT-over-expressing cell lines (top left panel). However, although high levels of UGT1A1 protein were still observed in the microsomal fraction, UGT1A10 protein levels were significantly decreased in the microsomes (top right panel). Using the endoplasmic reticulum-resident protein calnexin as a loading control (bottom panels), a

Table I. Glucuronidation rate of individual UGT family members against PhIP and *N*-OH-PhIP

UGT homogenate[a]	PhIP		*N*-OH-PhIP	
	N^2-Gluc[b]	N3-Gluc[b]	N^2-Gluc[b]	N3-Gluc[b]
1A1	0.34 ± 0.02	0.047 ± 0.004	21.7 ± 5.1	3.7 ± 0.9
1A3	ND	ND	0.59 ± 0.05	1.5 ± 0.2
1A4	0.006 ± 0.005	0.40 ± 0.28	7.1 ± 1.0	0.91 ± 0.20
1A6	ND	ND	ND	ND
1A7	ND	ND	0.21 ± 0.10	0.51 ± 0.20
1A8	ND	ND	2.5 ± 0.4	1.4 ± 0.7
1A9	0.02 ± 0.004	0.02 ± 0.01	1.1 ± 0.1	1.6 ± 0.3
1A10	2.7 ± 0.5	0.12 ± 0.01	152 ± 26	34.3 ± 6.1
2B4	ND	ND	ND	ND
2B7	ND	ND	ND	ND
2B10	ND	ND	ND	ND
2B11	ND	ND	ND	ND
2B15	ND	ND	ND	ND
2B17	ND	ND	ND	ND

[a]All reactions were performed using 0.3 mg protein of UGT-over-expressing cell homogenate and 125 μM substrate for 90 min at 37°C. Data are reported as mean ± standard deviation for three independent experiments. ND, not detected.

[b]Glucuronidation rates (pmol/min/μg UGT) are normalized to relative UGT expression in the individual UGT-over-expressing cell homogenates as determined by western blot analysis (Figure 2).

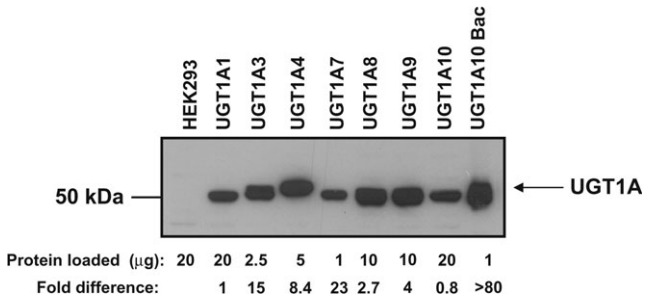

Fig. 2. Analysis of UGT1A expression. Representative western blot analysis of UGT1A protein levels in homogenate lysates from the individual UGT1A-over-expressing cell lines used in the glucuronidation activity analysis against PhIP and *N*-OH-PhIP. To obtain a single blot with densitometric readings on the linear part of the curve for all family 1A UGTs, varying amounts of total cellular protein were loaded: 20 μg of UGT1A1, 2.5 μg of UGT1A3, 5 μg of UGT1A4, 1 μg of UGT1A7, 10 μg of UGT1A8, 10 μg of UGT1A9 and 20 μg of UGT1A10; 1 μg of UGT1A10-over-expressing baculosomes were also loaded. The negative control HEK293 lane shows no UGT1A expression in the parental HEK293 cells. The relative expression of each UGT1A is shown under the blot, with the level of UGT1A1 protein arbitrarily set to 1.0. Fold-difference values are the average of three independent western blot experiments normalized to β-actin.

20-fold decrease in protein expression was observed for UGT1A10 in microsomes compared with only a 1.7-fold decrease for UGT1A1 (Figure 4), indicating that the majority of UGT1A10 protein does not reside in the microsomal fraction. A similar pattern of primarily microsomal compartmentalization exhibited by UGT1A1 was observed for UGTs 1A4, 1A6 and 1A9 (data not shown). These data suggest that, unlike that observed for other UGTs, UGT1A10 may not primarily reside in the microsomal fraction of cells and may explain why UGT1A10 activity against PhIP and *N*-OH-PhIP went undetected in previous studies.

To better assess the relative activity of UGT1A10 against *N*-OH-PhIP and to more fully evaluate differences in activity between homogenates from UGT1A10-over-expressing cells versus UGT1A10-over-expressing baculosomes, kinetic analysis was performed. Homogenates from cells over-expressing UGT1A10 exhibited 22- to 31-fold higher levels of glucuronidation activity than UGT1A1 cell homogenates in the formation of *N*-OH-PhIP-glucuronides as determined by V_{max}/K_M, reflecting decreases in K_M and increases in V_{max} (Table II). Although kinetic constants could not be calculated for UGT1A10 microsomes due to low UGT1A10 expression and correspondingly low glucuronidation activities, similar kinetics were observed for microsomes from UGT1A1-over-expressing cells as compared with UGT1A1 homogenates against *N*-OH-PhIP (Table II). This suggests that the high level of activity observed for UGT1A10 homogenates was not due to differences in homogenate versus microsome preparation. Consistent with previous studies suggesting that UGT-over-expressing baculosomes may not be optimal for activity assessments against all substrates (19), a 600- to 4700-fold decrease in V_{max}/K_M, reflected by an increase in K_M and a decrease in V_{max}, were observed for UGT1A10 baculosomes as compared with homogenates from UGT1A10-over-expressing cells in both N^2- and N3-glucuronide formation for *N*-OH-PhIP (Table II).

Kinetic analysis of wild-type UGT1A10^{139Glu} and polymorphic UGT1A10^{139Lys} against PhIP and N-OH-PhIP

To address potential inter-individual differences in glucuronidation rates against PhIP and *N*-OH-PhIP, kinetic analysis of UGT1A10 variants was performed. In previous studies, the African American-specific codon 139 variant of UGT1A10 (Glu > Lys) exhibited a 2-fold decrease in activity against all polycyclic aromatic hydrocarbons tested as compared with wild-type UGT1A10 as determined by V_{max}/K_M (19). In the present study, homogenates from cells over-expressing the UGT1A10^{139Lys} variant exhibited a significantly ($P < 0.01$) lower V_{max}/K_M against PhIP and *N*-OH-PhIP at both the N^2 and N3 positions as compared with the wild-type UGT1A10^{139Glu} isoform (Table III). Specifically, the wild-type UGT1A10^{139Glu} exhibited a 5.7- and 15.8-fold higher V_{max}/K_M for *N*-OH-PhIP-N^2-glucuronide and *N*-OH-PhIP-N3-glucuronide formation, respectively, and a 3- and 2.2-fold higher V_{max}/K_M for PhIP-N^2-glucuronide and PhIP-N3-glucuronide formation, respectively, than the UGT1A10^{139Lys} variant.

Discussion

UGT1A10 is an extra-hepatic enzyme that is expressed in several target tissues for polycyclic aromatic hydrocarbon- and HCA-induced cancers including the colon (23), aerodigestive tract (24) and lung (19). UGT1A10 has been implicated in the glucuronidation and detoxification of several carcinogens that play an important role in cancer initiation at these sites and was shown to be the most active UGT against several metabolites of BaP (19). The present study demonstrates that UGT1A10 is also the most active UGT *in vitro* against the HCA PhIP, and its bioactivated metabolite, *N*-OH-PhIP. This reinforces the hypothesis that the extra-hepatic UGT1A10 may play a critical role in the detoxification of pertinent carcinogens in these target tissues.

Previous studies examining UGT activity against HCAs had indicated that UGT1A10 exhibited little or no activity against either PhIP (5) or *N*-OH-PhIP (5,6,16). In a comprehensive screening study of most UGTs, Girard *et al.* (6) demonstrated that several UGT1A enzymes as well as UGT2B10 formed glucuronides of *N*-OH-PhIP; however, UGT1A10 exhibited no detectable activity against *N*-OH-PhIP in this study. This result may be due to the use of microsomal fractions of UGT-over-expressing cells when screening for activity against *N*-OH-PhIP in this study, since the current study demonstrates low levels of UGT1A10 are present in the microsomal fraction. The K_Ms for N^2- and N3-glucuronide formation exhibited by UGT1A1 microsomes as well as homogenates against *N*-OH-PhIP in the present study were similar to those reported previously (6), suggesting that the kinetic analysis performed in the present study was accurate and not a function of differences in cell homogenate versus cellular microsome preparations. While the UGTs are thought to reside primarily in the endoplasmic reticulum, one report has described the localization of UGTs 1A6 and 2B7 in the nucleus as well as the endoplasmic

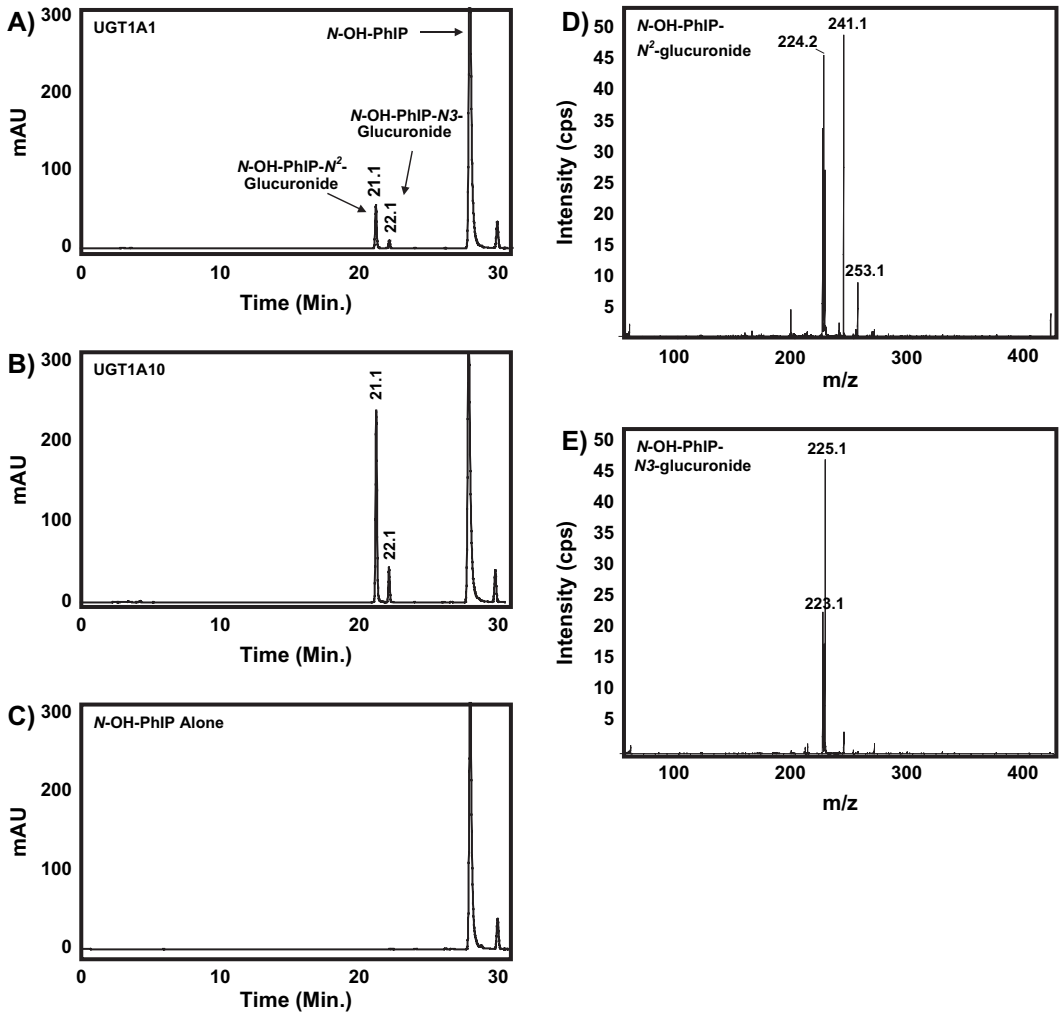

Fig. 3. Representative HPLC traces of *N*-OH-PhIP-glucuronide separation and detection. All assays were performed using 125 μM *N*-OH-PhIP and incubated for 90 min at 37°C. (**A**) HPLC trace using 300 μg protein of UGT1A1-over-expressing cell homogenates; *N*-OH-PhIP, *N*-OH-PhIP-N^2-glucuronide and *N*-OH-PhIP-N3-glucuronide are indicated. (**B**) HPLC trace using 300 μg protein of UGT1A10-over-expressing homogenates. (**C**) HPLC trace of *N*-OH-PhIP alone. (**D**) Mass spectral analysis of peak 1 (retention time 21.1 min). (**E**) Mass spectral analysis of peak 2 (retention time 22.1 min).

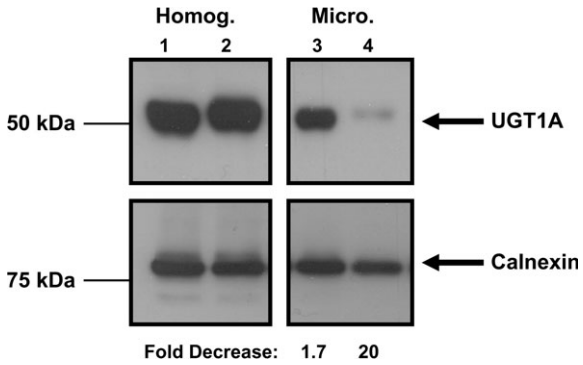

Fig. 4. Analysis of UGT1A1 and UGT1A10 expression in UGT-over-expressing HEK293 cell homogenates versus microsomal fractions. Western blot analysis of lysates (40 μg) from UGT1A1-over-expressing homogenates (lane 1) or microsomes (lane 3) and UGT1A10-over-expressing homogenates (lane 2) or microsomes (lane 4). The upper panels are probed with the UGT1A antibody and the bottom panels are probed with a calnexin antibody as a loading control. The fold decrease is shown below the figure comparing the UGT expression in lanes 3 to 1 and lanes 4 to 2 relative to calnexin as determined by densitometry.

reticulum (25), indicating that further study on UGT1A cellular localization is warranted.

In a prior study (16), UGT-over-expressing baculosomes were used for screening glucuronidation activities against *N*-OH-PhIP. As shown in the present study for UGT1A10, activity relationships between UGT-over-expressing baculosomes do not necessarily mimic that observed for UGT-over-expressing cell lines. This is consistent with previous studies demonstrating high activity for UGT1A10-over-expressing cell homogenates against benzo(a)pyrene metabolites whereas UGT1A10-over-expressing baculosomes exhibit relatively low activity against some of the same metabolites tested in previous studies (19,24). This variation in activity may be due to potential differences in post-translational modifications between the two systems. For example, dramatic differences in post-translational modifications such as N-glycosylation, C-terminal polypeptide cleavage and protein folding have been well documented between these two expression systems (26,27). Furthermore, phosphorylation was shown to be required for UGT1A10 activity for a variety of substrates (28), a post-translational modification that may differ between mammalian and insect cells. Therefore, the high glucuronidation activity of UGT1A10 against *N*-OH-PhIP may not have been detected in previous studies due to either low UGT1A10 expression in microsomal fractions (6) or differences in activity when over-expressing UGT1A10 in baculosomes (16).

Another difference between the present study and previous reports was the lack of formation of uncharacterized *N*-OH-PhIP-glucuronide

Table II. Kinetic analysis of glucuronide formation for *N*-OH-PhIP comparing UGT1A-over-expressing cell homogenates versus corresponding cellular microsomal fraction or UGT1A10-over-expressing baculosomes

UGT[a]	N^2-glucuronide			N3-glucuronide		
	K_M (μM)	V_{max}[b] (pmol/min/μg)	V_{max}/K_M[b] (μl/min/μg)	K_M (μM)	V_{max}[b] (pmol/min/μg)	V_{max}/K_M[b] (μl/min/μg)
1A1 homogenate	16.6 ± 1.9	42.2 ± 9.5	2.5 ± 0.6	48.4 ± 11.2	39.5 ± 12.2	0.82 ± 0.19
1A1 microsomes	19.4 ± 10.0	39.1 ± 7.5	2.0 ± 0.5	10.8 ± 6.1	28.7 ± 6.2	2.7 ± 1.2
1A10 homogenate	3.2 ± 0.9	178 ± 23	55.6 ± 9.5	6.7 ± 3.5	169 ± 92	25.2 ± 6.1
1A10 baculosomes	75.9 ± 11.2	0.93 ± 0.05	0.012 ± 0.002	64.2 ± 15.5	2.3 ± 0.6	0.04 ± 0.02

[a]All reactions were performed using 20 μg of UGT1A-over-expressing cell extract and incubated for 30 min at 37°C. Kinetic data are reported as mean ± standard deviation for three independent experiments.
[b]V_{max} values are adjusted per microgram of the corresponding UGT1A protein as determined by western blot analysis (Figure 2).

Table III. Kinetic analysis of PhIP- and *N*-OH-PhIP-glucuronide formation comparing UGT1A10^{139Glu}-and UGT1A10^{139Lys}-over-expressing cell homogenates

Substrate	UGT1A10^{139Glu}			UGT1A10^{139Lys}		
	K_M (μM)	V_{max}[a] (pmol/min/μg)	V_{max}/K_M[a] (μl/min/μg)	K_M (μM)	V_{max}[a] (pmol/min/μg)	V_{max}/K_M[a] (μl/min/μg)
PhIP						
N^2-glucuronide	62.4 ± 12.4	7.6 ± 0.5	0.12 ± 0.017	414 ± 159	18.0 ± 3.4	0.04 ± 0.009[b]
N3-glucuronide	174 ± 54	5.7 ± 0.8	0.033 ± 0.006	941 ± 186	14.5 ± 1.7	0.015 ± 0.002[b]
N-OH-PhIP						
N^2-glucuronide	3.2 ± 0.9	178 ± 23	55.6 ± 9.5	10.9 ± 4.8	107 ± 33	9.8 ± 2.2[b]
N3-glucuronide	6.7 ± 3.5	169 ± 92	25.2 ± 6.1	16.9 ± 4.5	26.2 ± 3.6	1.6 ± 0.3[b]

[a]All reactions were performed using 20 μg UGT1A10-over-expressing cell homogenate and incubated for 30 min at 37°C. Kinetic data are reported as mean ± standard deviation for three independent experiments. V_{max} values are adjusted per microgram of the corresponding UGT1A protein as determined by western blot (Figure 2).
[b]Significant ($P < 0.01$) decrease in kinetic parameter observed for homogenates from UGT1A10^{139Lys}- versus UGT1A10^{139Glu}-over-expressing cells.

peaks in assays performed for UGT-over-expressing cell lines in the present study. Specifically, no activity was observed in this study for UGT2B10 against *N*-OH-PhIP which seemingly contradicts a previous report that UGT2B10 formed an uncharacterized glucuronide termed 'Glucu 2' (6). In this same report, UGT1A9 was also shown to yield Glucu 2 as well as the N^2- and N3-glucuronides of *N*-OH-PhIP (6). In the current report, UGT1A9 was observed to produce only the N^2- and N3-glucuronides of *N*-OH-PhIP. This is likely due to Glucu 2 formation being detected by the HPLC-mass spectrometry/mass spectrometry (LC-MS/MS) methodology employed in the previous study but was below the detection limit of the HPLC-ultraviolet analysis performed in the present study for the over-expressing lines.

Recent studies have demonstrated that the levels of urinary *N*-OH-PhIP-N^2-glucuronide, the major PhIP metabolite detected, was inversely correlated with DNA adduct levels in colonic cells in subjects who consumed doses of PhIP that were comparable with that of a diet high in HCAs (7). Interestingly, significant levels of *N*-OH-PhIP-N3-glucuronide and PhIP-N^2-glucuronide were also observed in urine. This indicates that glucuronidation is a major detoxification mechanism for PhIP in humans. These studies further suggested that variations in the levels of glucuronidation between individuals could substantially influence risk for HCA-induced adducts and therefore cancer risk. Since UGT1A10 exhibited the highest activity of any UGT toward both PhIP and *N*-OH-PhIP, functional variations in this gene could play an important role in susceptibility to PhIP-induced carcinogenesis. The UGT1A10^{139Lys} variant isoform exhibited significantly decreased activity against both PhIP and *N*-OH-PhIP as compared with the wild-type UGT1A10^{139Glu} isoform in the present study. This is consistent with the decreased activity observed for this variant against several polycyclic aromatic hydrocarbons in previous studies (19). Taken together, individuals with the UGT1A10^{139Lys} variant allele may be increasingly susceptible to exposures from a variety of carcinogens and may be at increased risk for colorectal carcinoma in particular. Genotyping of this polymorphism within large colon cancer case–control studies will be necessary to directly test this hypothesis.

In summary, the evidence presented here indicates that UGT1A10 is the most efficient detoxifier of the carcinogen PhIP and its bioactivated metabolite *N*-OH-PhIP and that the UGT1A10^{139Lys} polymorphism exhibited significantly reduced activity against PhIP and *N*-OH-PhIP. These studies suggest that functional variants within the UGT1A10 gene may be important risk factors for colorectal cancer.

Funding

National Institutes of Health, Department of Health and Human Services [Public Health Service grants R01-DE13158 (National Institute for Dental and Craniofacial Research) and P01-CA68384 (National Cancer Institute)] to P.L.; two formula grants under the Pennsylvania Department of Health, Health Research Formula Funding Program (State of PA, Act 2001-77-part of the PA tobacco settlement legislation) to P.L. and S.A.

Acknowledgements

We thank Dongxiao Sun for technical assistance and scientific discussions as well as the Macromolecular Core Facility at the Penn State University College of Medicine for usage of densitometric equipment. We also thank Jenny Dai in the Mass Spectrometer Core Facility at the Penn State University College of Medicine for technical assistance.

Conflicts of Interest Statement: None declared.

References

1. Felton,J.S. *et al*. (1986) The isolation and identification of a new mutagen from fried ground beef: 2-amino-1-methyl-6-phenylimidazo[4,5-b]pyridine (PhIP). *Carcinogenesis*, **7**, 1081–1086.
2. Skog,K.I. *et al*. (1998) Carcinogenic heterocyclic amines in model systems and cooked food: a review on formation, occurrence and intake. *Food Chem. Toxicol.*, **36**, 879–896.

3. Manabe,S. *et al*. (1991) Detection of a carcinogen, 2-amino-1-methyl-6-phenylimidazo[4,5-b]pyridine (PhIP), in cigarette smoke condensate. *Carcinogenesis*, **12**, 1945–1947.
4. Nakagama,H. *et al*. (2005) Modeling human colon cancer in rodents using a food-borne carcinogen, PhIP. *Cancer Sci.*, **96**, 627–636.
5. Malfatti,M.A. *et al*. (2001) N-Glucuronidation of 2-amino-1-methyl-6-phenylimidazo[4,5-b]pyridine (PhIP) and *N*-hydroxy-PhIP by specific human UDP-glucuronosyltransferases. *Carcinogenesis*, **22**, 1087–1093.
6. Girard,H. *et al*. (2005) UGT1A1 polymorphisms are important determinants of dietary detoxification in the liver. *Hepatology*, **42**, 448–457.
7. Malfatti,M.A. *et al*. (2006) The urinary metabolite profile of the dietary carcinogen 2-amino-1-methyl-6-phenylimidazo[4,5-b]pyridine is predictive of colon DNA adducts after low-dose exposure to humans. *Cancer Res.*, **66**, 10541–10547.
8. Tephly,T.R. *et al*. (1990) UDP-glucuronosyltransferases: a family of detoxifying enzymes. *Trends Pharmacol. Sci.*, **11**, 276–279.
9. Owens,I.S. *et al*. (1995) Gene structure at the human UGT1 locus creates diversity in isozyme structure, substrate specificity, and regulation. *Prog. Nucleic Acid Res. Mol. Biol.*, **51**, 305–338.
10. Gueraud,F. *et al*. (1998) Glucuronidation: a dual control. *Gen. Pharmacol.*, **31**, 683–688.
11. Ren,Q. *et al*. (2000) O-Glucuronidation of the lung carcinogen 4-(methylnitrosamino)-1-(3-pyridyl)-1-butanol (NNAL) by human UDP-glucuronosyltransferases 2B7 and 1A9. *Drug Metab. Dispos.*, **28**, 1352–1360.
12. Tukey,R.H. *et al*. (2000) Human UDP-glucuronosyltransferases: metabolism, expression, and disease. *Annu. Rev. Pharmacol. Toxicol.*, **40**, 581–616.
13. Nagar,S. *et al*. (2006) Uridine diphosphoglucuronosyltranferase pharmacogenetics and cancer. *Oncogene.*, **25**, 1659–1672.
14. Jin,C.J. *et al*. (1993) Complementary deoxyribonucleic acid cloning and expression of a human liver uridine diphosphate-glucuronosyltransferase glucuronidating carboxylic acid-containing drugs. *J. Pharmacol. Exp. Ther.*, **264**, 475–479.
15. Beaulieu,M. *et al*. (1997) Chromosomal localization, structure, and regulation of the UGT2B17 gene, encoding a C19 steroid metabolizing enzyme. *DNA Cell Biol.*, **16**, 1143–1154.
16. Malfatti,M.A. *et al*. (2004) Human UDP-glucuronosyltransferase 1A1 is the primary enzyme responsible for the N-glucuronidation of *N*-hydroxy-PhIP *in vitro*. *Chem. Res. Toxicol.*, **17**, 1137–1144.
17. Kulp,K.S. *et al*. (2000) Identification of urine metabolites of 2-amino-1-methyl-6-phenylimidazo[4,5-*b*]pyridine following consumption of a single cooked chicken meal in humans. *Carcinogenesis*, **21**, 2065–2072.
18. Wiener,D. *et al*. (2004) UDP-glucuronosyltransferase 1A4: *N*-glucuronidation of the lung carcinogen 4-(methylnitrosamino)-1-(3-pyridyl)-1-butanol (NNAL). *Drug Metab. Dispos.*, **32**, 72–79.
19. Dellinger,R.W. *et al*. (2006) Importance of UDP-glucuronosyltransferase 1A10 (UGT1A10) in the detoxification of polycyclic aromatic hydrocarbons: decreased glucuronidative activity of the UGT1A10^{139Lys} isoform. *Drug Metab. Dispos.*, **34**, 943–949.
20. Sun,D. *et al*. (2006) Characterization of tamoxifen and 4-hydroxytamoxifen glucuronidation by human UGT1A4 variants. *Breast Cancer Res.*, **8**, R50.
21. Fang,J.-L. *et al*. (2002) Characterization of benzo[*a*]pyrene-7,8-dihydrodiol glucuronidation by human liver microsomes and over-expressed human UDP-glucuronosyltransferase enzymes. *Cancer Res.*, **62**, 1978–1986.
22. Wiener,D. *et al*. (2004) Correlation between UDP-glucuronosyl-transferase genotypes and NNAL glucuronidation phenotype in human liver microsomes. *Cancer Res.*, **64**, 1190–1196.
23. Strassburg,C.P. *et al*. (1999) UDP-glucuronosyltransferase activity in human liver and colon. *Gastroenterology*, **116**, 149–160.
24. Zheng,Z. *et al*. (2002) Glucuronidation: an important mechanism for detoxification of benzo[a]pyrene metabolites in aerodigestive tract tissues. *Drug Metab. Dispos.*, **30**, 397–403.
25. Radominska-Pandya,A. *et al*. (2002) Nuclear UDP-glucuronosyltransferases: identification of UGT2B7 and UGT1A6 in human liver nuclear membranes. *Arch. Biochem. Biophys.*, **399**, 37–48.
26. James,D.C. *et al*. (1996) Posttranslational processing of recombinant human interferon-gamma in animal expression systems. *Protein Sci.*, **5**, 331–340.
27. Sun,J. *et al*. (2006) Structural and functional analysis of the human Toll-like receptor 3. Role of glycosylation. *J. Biol. Chem.*, **281**, 11144–11151.
28. Basu,N.K. *et al*. (2005) Phosphorylation of UDP-glucuronosyltransferase regulates substrate specificity. *Proc. Natl Acad. Sci. USA*, **102**, 6285–6290.

Received March 7, 2007; revised June 29, 2007; accepted July 6, 2007